Ⅲ. 資　　料

4）慢性肉芽腫症に対する遺伝子治療の実績一覧

慢性肉芽腫症に対する遺伝子治療の実績一覧

2008年12月現在

症例	年齢	病型	実施国	実施時期	導入細胞	ベクター	前処置	効果	経過
1	26	gp91	ドイツ	2004	PBSC	SF71gp91phox	BU 8mg/kg	あり	死亡 (Mono7)
2	25	gp91	ドイツ	2003	PBSC	SF71gp91phox	BU 8mg/kg	あり	移植 (MDS)
3	5	gp91	スイス	2003	PBSC	SF71gp91phox	BU 8mg/kg	あり	生 (1.0%)
4	8	gp91	スイス	2008	PBSC	SF71gp91phox	BU 8mg/kg	あり	生 (90%)
5	12	gp91	イギリス	2001	PBSC	MFGS-gp91phox	Mel 140mg/kg	あり	生 (<0.1)
6	27	gp91	イギリス	2005	BMSC	SF71gp91phox	Mel 140mg/kg	なし	生 (<0.1)
7	6	gp91	イギリス	2006	PBSC	SF71gp91phox	Mel 140mg/kg	なし	生 (<0.1)
8	9	gp91	イギリス	2007	PBSC	SF71gp91phox	Mel 140mg/kg	あり	生 (<0.1)
9	16	gp91	韓国	2006	PBSC	MT-gp91	BU 8mg/kg	-	生 (<0.1)
10	9	gp91	韓国	2006	PBSC	MT-gp91	BU 8mg/kg	-	生 (<0.1)
11-15	37F 21M 18F 27M 27F	p47	米国	1995～	PBSC	MFGS-p47phox	なし	なし	生
16	20	gp91	米国	1998～2000	PBSC	MFGS-gp91phox	なし	なし	生
17-20	未発表	gp91	米国	1998～2000	PBSC	MFGS-gp91phox	なし	なし	生
21	28	gp91	米国	2006～	PBSC	MFGS-gp91phox	BU 10mg/kg	あり	生 (<1)
22	31	gp91	米国	2006～	PBSC	MFGS-gp91phox	BU 10mg/kg	なし	死亡(感染症)
23	37	gp91	米国	2008～	PBSC	MFGS-gp91phox	BU 10mg/kg	あり	生

・PBSC：G-CSF誘導末梢血由来CD34陽性細胞、BMSC：骨髄由来CD34陽性細胞
・SF71pg91phox： spleen focus forming virus由来レトロウイルスベクター
・MFGSgp91phox、MT-gp91： MoMLV由来レトロウイルスベクター
・BU：ブスルファン、Mel： メルファラン

Ⅳ．研究成果の刊行に関する一覧表

研究成果の刊行に関する一覧表

雑 誌

発表者氏名	論文タイトル名	発表誌名	巻号	ページ	出版年
Tamase A, Muraguchi T, Naka K, Hoshii T, Ohmura M, Kinoshita M, Tanaka S, Shugo H, Ooshio T, Nakada M, Sawamoto K, Onodera M, Matsumoto K, Oshima M, Asano M, Saya H, Okano H, Suda T, Hamada J, Hirao A	Identification of tumor-initiating cells in a highly aggressive brain tumor using promoter activity of nucleostemin.	PNAS	106(40)	17163-17168	2009
Okabe M, Otsu M, Ahn DH, Kobayashi T, Morita Y, Wakiyama Y, Onodera M, Eto K, Ema H, Nakauchi H.	Definitive proof for direct reprogramming of hematopoietic cells to pluripotency.	Blood	114(9)	1764-1767	2009
Miyamoto N, Tanaka R, Zhang N, Shimura H, Onodera M, Mochizuki H, Hattori N, Urabe T.	Crucial role for pCREB signaling in the differentiation and survival of neural progenitors under chronic cerebral hypoperfusion.	Neuroscience	162(2)	525-536	2009
Fujisawa Y, Nabekura T, Nakao T, Nakamura Y, Takahashi T, Kawachi Y, Otsuka F, Onodera M:	The induction of tumor-specific CD4+ T cells via major histocompatibility complex class II is required to gain optimal anti-tumor immunity against B16 melanoma cell line in tumor immunotherapy using dendritic cells.	Exp Dermatol	18(4)	396-403	2009
小野寺雅史	造血幹細胞を標的とした遺伝子治療の開発	ゲノム医学		3943-3946	2009
小野寺雅史	小児における遺伝子治療	小児科	50	828-833	2009
Horiuchi Y, Onodera M, Miyagawa Y, Sato B, Onda K, Katagiri YU, Okita H, Okada M, Otsu M, Kume A, Okuyama T, Fujimoto J, Kuratsuji T, Kiyokawa N.	Kinetics and Effect of Integrin Expression on Human CD34(+) Cells during Murine Leukemia Virus-Derived Retroviral Transduction with Recombinant Fibronectin for Stem Cell Gene Therapy.	Hum Gene Ther	20(7)	777-873	2009

Miyagawa Y, Kiyokawa N, Ochiai N, Imadome K-I, Horiuchi Y, Onda K, Yajima M, Nakamura H, Katagiri YU, Okita H, Morio T, Shimizu N, Fujimoto J, Fujiwara S.	Ex vivo expanded cord blood CD4 T lymphocytes exhibit distinct expression profile of cytokine-related genes from those of peripheral blood origin. Immunology.	Immunology	128(3)	405-419	2009
Morita M, Fujino M,Jiang GP, Kitazawa Y, Xie L, Azuma M,Yagita H, Nagao S, Sugioka A, Kurosawa Y, Takahara S, Fung J, Qian S, Lu L, Li X-K.	PD1/B7-H1 interaction contribute to thespontaneousacceptance of mouse liverallograf	Am J Transplant .	10(1)	40-46	2010
Kitazawa Y, Fujino M, Li X-K*, Xie L, Ichimaru N, Okumi M, Nonomura N, Tsujimura A, Isaka Y, Kimura H, Hunig T, Takahara S.	Superagonist CD28 antibody preferentially expanded Foxp3-expressing nTreg cells and prevented graft-versus-host diseases	Cell Transplant	118(5)	627-637	2009
Xie L, Li X-K*, Funeshima-Fuji N, Kimura H, Matsumoto Y, Isaka Y, Takahara S.	Amelioration of experimental autoimmune encephalomyelitis by curcumin treatment through inhibition of IL-17 production.	Int Immunopharmacol	9(5)	575-581	2009
Pan XC, Deng YB, Sugawara Y, Makuuchi M, Okabe M, Ochiya T, Sugiura W, Kitazawa Y, Fuji N, Li X-K, Miyamoto M, Kimura H.	Immunological behavior of enhanced green fluorescent protein (EGFP) as a minor histocompatibility antigen with a special reference to skin isograft and specific regulation of local graft-versus-host reaction (GvHR).	Immunol Lett	123(2)	103-113	2009
Tsuji A.B, Morita M, Li X-K*, Sogawa C, Sudo H, Sugyo A, Fujino M, Sugioka A, Koizumi M, Saga T.	18F-FDG PET for the SemiquantitativeEvaluation of AcuteAllograft Rejection and the Immunosuppression Therapy Efficacy in Liver Transplantation Rat Models.	J Nucl Med	50(5)	827-830	2009
Funeshima-Fuji N, Fujino M, Xie L, Kimura H, Takahara S, Ezaki T, Zhu BT, Li X-K.	Prolongation of rat major histocompatibility complex-compatible cardiac allograft survival during pregnancy.	J Heart Lung Transplant	28(2)	176-182	2009

Okuyama T, TanakaA, Suzuki Y, Ida H, Tanaka T,Cox GF, Eto Y,Orii T.	Japan Elaprase((R)) Treatment (JET)study:Idursulfaseenzyme replacement therapy in adult patients with attenuated Huntersyndrome (MucopolysaccharidosisII, MPS II).	Molecular genetics and metabolism	99	18-25	2010
Nakajima M, Yamada M, Yamaguchi K, Sakiyama Y, Oda A, Nelson DL, Yawaka Y, Ariga T.	Possible application of flow cytometry for evaluation of the structure and functional status of WASP in peripheral blood mononuclear cells.	Eur J Haematol	82(3)	223-230	2009
Maekawa K, Yamada M, Okura Y, Sato Y, Yamada Y, Kawamura N, Ariga T.	X-linked agammaglobulinemia in a 10-year-old boy with a novel non-invariant splice-site mutation in *Btk* gene.	Blood Cell Mol. Dis.			in press
Kato I, Umeda K, Awaya T, Yui Y, Niwa A, Fujino H, Matsubara H, Watanabe K, Heike T, Adachi N, Endo F, Mizukami T, Nunoi H, Nakahata T, Adachi S.	Successful treatment of refractory donor lymphocyte infusion-induced immune-mediated pancytopenia with rituximab.	Pediatr Blood Cancer	54(2)	329-331	2010
Moritake H, Ikeda T, Manabe A, Kamimura S, Nunoi H.	Cytomegalovirus infection mimicking juvenile myelomonocytic leukemia showing hypersensitivity to granulocyte-macrophage colony stimulating factor.	Pediatr Blood Cancer	53(7)	1324-1326	2009
Kawachi S, Luong ST, Shigematsu M, Furuya H, Phung TT, Phan PH, Nunoi H, Nguyen LT, Suzuki K.	Risk parameters of fulminant acute respiratory distress syndrome and avian influenza (H5N1) infection in Vietnamese children.	J Infect Dis	200(4)	510-515	2009
Kawaguchi H, Okamoto S, Sikdar D, Kume A, Li F, Mohafez OM, Shehata MH, Hiraga K	Genomic organization of regions that regulate chicken glycine decarboxylase gene transcription: Physiological and pathological conditions.	Gene	432(1)	7-18	2009
Uchibori R, Okada T, Ito T, Urabe M, Mizukami H, Kume A, Ozawa K	Retroviral vector-producing mesenchymal stem cells for targeted suicide cancer gene therapy.	J Gene Med	11(5)	373-381	2009

Sanada M, Suzuki T, Shih LY, Otsu M, Kato M, Yamazaki S, Tamura A, Honda H, et al	Gain-of-function of mutated C-CBL tumour suppressor in myeloid neoplasms.	Nature	460(7257)	904-908	2009
Nishimura S, Manabe I, Nagasaki M, Eto K, Yamashita H, Ohsugi M, Otsu M, Hara K, Ueki K, Sugiura S, Yoshimura K, Kadowaki T, Nagai R.	CD8+ effector T cells contribute to macrophage recruitment and adipose tissue inflammation in obesity.	Nat Med	15(8)	914-920	2009
Ogaeri T, Eto K, Otsu M, Ema H, Nakauchi H.	The actin polymerization regulator WAVE2 is required for early bone marrow repopulation by hematopoietic stem cells.	Stem Cells	27 (5)	1120-1129	2009
Sogo T, Kawahara M, Ueda H, Otsu M, Onodera M, Nakauchi H, Nagamune T.	T cell growth control using hapten-specific antibody/interleukin-2 receptor chimera.	Cytokine.	46(1)	127136	2009

書　籍

著者氏名	論文タイトル名	書籍全体の編集者名	書　籍　名	出版社名	出版地	出版年	ページ
有賀　正	全身に見られる症候　易感染症	金澤一郎、永井良三	今日の診断指針第六版	医学書院、	東京都	印刷中	
有賀　正	原発性免疫不全症私はこう治療している。		今日の治療指針　2011年度版	医学書院	東京都	印刷中	

学会発表

発表者氏名	タイトル名	学会名	場所	開催日
Horiuchi Y, Onodera M, Miyagawa Y, Sato B, Onda K, Katagiri YU, Okita H, Okada M, Otsu M, Kume A, Okuyaka T, Fujimoto J, Kuratsuji T, Kiyokawa N	Kinetics and defect of integrin expression on human CD34+ cells during MLV-derived retroviral transduction with a recombinant fibronectin for stem cell gene therapy.	第 15 回日本遺伝子治療学会	吹田	2009. 7.9-11
Tadokoro K, Azuma N, Onodera M.	A reciprocal regulation between PAX2 and PAX6.	The 32nd Annual Meeting of the Molecular Biology Society of Japan, Japan	Yokohama	2009.12.9-12
Takeuchi Y, Otsu M, Onodera M, Nakauchi H	A threshold in expression levels of gp91phox transgene limits the degree of functional correction in granulocytes after gene therapy for X-CGD	XVIIth Annual Congress of the European Society of Gene and Cell Therapy	Hannover, Germany	2009. 11.20-25
Takeuchi Y, Otsu M, Onodera M, Nakauchi H	Preclinical studies to improve the efficacy of stem cell gene therapy for X-CGD	XVth Annual Meeting of the Japanese Society of Gene Therapy	Osaka	2009. 9.11-12
小野寺雅史	小児難治性疾患に対する遺伝子細胞治療の発展に向けて。	第 9 回 小児免疫リウマチ研究会	東京	2009. 4.10
小野寺雅史	我が国における遺伝子医薬品承認に向けての課題と取組み。	第 8 回 遺伝子治療シンポジウム、	大阪	2010. 2.5
Kiyokawa N, Onda K, Imadome K-I, Yajima M, Nakamura H, Katagiri YU, Morio T, Fujimoto J, Fujiwara S.	Ex vivo expanded cord blood CD4 T lymphocytes exhibit a distinct expression profile of cytokine-related genes from those of peripheral blood origin.	第 39 回日本免疫学会学術集会	大阪	2009. 12.2-4
Okuyama T, Tanaka A, Suzuki Y, Ida H, Tanaka T, Cox GF, Eto Y, Orii T.	Idursulfase enzyme replacement therapy in adult patients with attenuated Hunter syndrome (Mucopolysaccharidosis II, MPS II). Mol Genet Metab	Japan Elaprase((R)) Treatment (JET) study		2009. 8.24

有賀　正	Wiskott-Aldrich 症候群の病態・診断・治療・トピックス	北海道免疫不全講演会	札幌	2009. 7.24
有賀　正	原発性免疫不全症に対する遺伝子治療の現状と問題点	第 16 回日本遺伝子診療学会	札幌	2009. 7.31
久米晃啓、八木洋也、小倉剛、水上浩明、卜部匡司、小澤敬也	改良型アデノ随伴ウイルスベクターによるフェニルケトン尿症遺伝子治療	第 112 回日本小児科学会小児科学会学術集会	奈良	2009. 4.17-19
Yagi H, Sanechika S, Ichinose H, Mizukami H, Ogura T, Urabe M, Hamada H, Yoshikawa H, Ozawa K, Kume A	Improvement of monoamine metabolism in phenylketonuria mouse brain treated with a self- complementary adeno-associated vector.	The 12th Annual Meeting of American Society of Gene and Cell Therapy	San Diego, USA	2009. 5.27-30
Iwata-Okada M, Okuyama T, Kobayashi S, Kawai T, Horiuchi Y, Kiyakawa N, Li XK, Fujimoto J, Otsu M, Kume A, ArigaT, Mizukami T, Nunoi H, Kuratsuji T, Malech HL, Kang EM, Onodera M	A report of the progressfor X-linked CGD gene therapy in Japan.	第 15 回日本遺伝子治療学会	吹田	2009. 7.9-11
Yagi H, Sanechika S, Ichinose H, Mizukami H, Ogura T, Urabe M, Hamada H, Yoshikawa K, Ozawa K, Kume A	Liver- targeted gene therapy with a self- complementary AAV ameliorated brain aminergic deficit in phenylketonuria mice.	第 15 回日本遺伝子治療学会	吹田	2009. 7.9-11
久米晃啓、八木洋也、水上浩明、卜部匡司、塚原智典、実近翔、一瀬宏、小澤敬也	フェニルケトン尿症遺伝子治療による神経伝達モノアミン代謝の改善.	日本人類遺伝学会第 54 回大会	東京	2009. 9.23-26

Kume A, Yagi H, Mizukami H, Urabe M, Tsukahara T, Ishiwata A, Mimuro J, Madoiwa S, Ohmori T, Sakata Y, Ozawa K	Promoter selection for muscle-directed self-complementary AAV toward hemophilia B gene thearapy.	第 71 回日本血液学会学術集会	京都	2009. 10.23-25
Kume A, Yagi H, Sanechika S, Ichinose H, Mizukami H, Urabe M, Ozawa K	Liver-targeted gene therapy with a self-complementary AAV ameliorates brain aminergic deficit in phenylketonuria mice.	XVIIth Annual Congress of the European Society of Gene and Cell Therapy	Hannover, Germany	2009. 11.20-25
Suzuki S, Otsu M, Nakauchi H	Irradiated bone marrow environment affects HSC functions in hematopoietic stem cell transplantation.	71th Annual Meeting of the Japanese Society of Hematology	Kyoto	2009. 10.23-25
Takeuchi Y, Otsu M, Nakauchi H	Functional reconstitution in X-CGD mice established by allogeneic BMT with the use of anti-CD40L mAb	71th Annual Meeting of the Japanese Society of Hematology	Kyoto	2009. 10.23-25
Okabe M, Otsu M, Nakauchi H	Generation of iPS cells from Murine Marrow Hematopoietic cells	71th Annual Meeting of the Japanese Society of Hematology	Kyoto	2009. 10.23-25
大津　真	先天性免疫不全症の遺伝子細胞治療	第 37 回日本臨床免疫学会	東京	2009. 11.14

Ⅴ．　研究成果の印刷物・別刷

Identification of tumor-initiating cells in a highly aggressive brain tumor using promoter activity of nucleostemin

Akira Tamase[a,b,1], Teruyuki Muraguchi[a,1], Kazuhito Naka[a,1], Shingo Tanaka[a,b], Masashi Kinoshita[b], Takayuki Hoshii[a], Masako Ohmura[a], Haruhiko Shugo[a], Takako Ooshio[a,c], Mitsutoshi Nakada[b], Kazunobu Sawamoto[d], Masafumi Onodera[e], Kunio Matsumoto[f], Masanobu Oshima[g], Masahide Asano[h], Hideyuki Saya[i], Hideyuki Okano[j], Toshio Suda[k], Jun-ichiro Hamada[b], and Atsushi Hirao[a,c,2]

[a]Division of Molecular Genetics, Center for Cancer and Stem Cell Research, Cancer Research Institute, Kanazawa University, Kanazawa, Ishikawa 920-0934, Japan; [b]Department of Neurosurgery, Graduate School of Medical Science, Kanazawa University, Kanazawa, Ishikawa 920-8641, Japan; [c]Core Research for Evolutional Science and Technology, Japan Science and Technology Agency, Kawaguchi, Saitama 332-0012, Japan; [d]Department of Developmental and Regenerative Biology, Institute of Molecular Medicine, Nagoya City University Graduate School of Medical Sciences, Mizuho-ku, Nagoya 467-8601, Japan; [e]Laboratory of Genetic Diagnosis and Gene Therapy, Department of Genetics, National Research Institute for Child Health and Development, Setagaya-ku, Tokyo 157-8535, Japan; [f]Division of Tumor Dynamics and Regulation and [g]Division of Genetics, Cancer Research Institute and [h]Division of Transgenic Animal Science, Advanced Science Research Center, Kanazawa University, Kanazawa, Ishikawa, 920-8640, Japan; and [i]Division of Gene Regulation, Institute for Advanced Medical Research and Departments of [j]Physiology and [k]Cell Differentiation, The Sakaguchi Laboratory of Developmental Biology, Keio University School of Medicine, Shinjuku-ku, Tokyo 160-8582, Japan

Edited by Tak Wah Mak, Princess Margaret Hospital, Toronto, Canada, and approved August 12, 2009 (received for review May 7, 2009)

Controversy remains over whether the cancer stem cell (CSC) theory applies to all tumors. To determine whether cells within a highly aggressive solid tumor are stochastically or hierarchically organized, we combined a reporter system where the nucleostemin (NS) promoter drives GFP expression (termed NS-GFP) with a mouse brain tumor model induced by retroviral Ras expression on a $p16^{Ink4a}$/$p19^{Arf}$-deficient background. The NS-GFP system allowed us to monitor the differentiation process of normal neural stem/precursor cells by analyzing GFP fluorescence intensity. In tumor-bearing mice, despite the very high frequency of tumorigenic cells, we successfully identified the NS-GFP$^+$ cells as tumor-initiating cells (T-ICs). The clonal studies conclusively established that phenotypical heterogeneity can exist among the cells comprising a genetically homogeneous tumor, suggesting that this aggressive brain tumor follows the CSC model. Detailed analyses of the NS-GFP$^+$ brain tumor cells revealed that T-ICs showed activation of the receptor tyrosine kinase c-Met, which functions in tumor invasiveness. Thus, the NS-GFP system provides a powerful tool to elucidate stem cell biology in normal and malignant tissues.

cancer stem cell | invasion

Recent improvements in cell purification and transplantation techniques have contributed to the identification of cell populations known as tumor-initiating cells (T-ICs). These findings led to the idea that tumors are organized as hierarchies of cells sustained by such T-ICs, conceptually termed cancer stem cells (CSCs) (1, 2). Supporting this idea, in vivo models in which leukemia is initiated from primary human hematopoietic cells revealed that disease is sustained by leukemia-initiating cells (L-ICs) and that the L-ICs retain both myeloid and lymphoid lineage potential (3). Although many human malignancies appear to contain only rare tumorigenic cells or T-ICs when transplanted into NOD/SCID mice (4–6), the question of whether NOD/SCID assays underestimate the frequency of human tumorigenic cells due to differences between human and murine tissues has been raised. Recently, Quintana et al. (7) reported that ≈25% of unselected human melanoma cells from patients formed tumors when transplanted into highly immunocompromised NOD/SCID interleukin-2 receptor gamma chain null ($Il2r\gamma^{-/-}$) mice, in contrast to the very few T-ICs identified when the melanoma cells were transplanted into NOD/SCID mice (6). These results suggest that cells comprising human melanomas may constitute a homogeneous population and that any melanoma cells can form a tumor, i.e., that a hierarchical organization of tumor cells does not exist. Alternatively, it is also possible that, although T-IC frequency is very high in the melanoma, a true hierarchy exists in the aggressive tumor, because 75% of the tumor cells lack T-IC activity. It therefore remains controversial whether the cancer stem cell theory applies to all tumors (2). In our study, we have attempted to resolve this issue by examining the frequency of tumorigenic cells present in a highly aggressive murine solid tumor orthotopically transplanted into recipient mice. Our approach thus avoids the underestimation of tumorigenic cell frequency that might arise due to environmental differences between human and mouse tissues.

To investigate whether murine brain tumors exhibit cellular heterogeneity, we took advantage of our unique NS-GFP stem cell-marking system, in which the green fluorescent protein (GFP) is expressed under the control of promoter of the nucleostemin (NS) gene (8). The NS, a nucleolar GTPase, is found at high levels in various tissue stem cells and cancer cells (9). Because NS expression decreases rapidly in stem cells when these cells differentiate before cell cycle exit, it has been suggested that the NS protein is a marker for proliferating cells in an early multipotential state (9, 10). In the regenerating newt lens, the NS protein rapidly accumulates in the nucleoli of dedifferentiating pigmented epithelial cells (11), suggesting that NS expression correlates with undifferentiated status of cells. Previously, we generated NS-GFP transgenic (NS-GFP-Tg) mice and used these mice to identify a fraction of neonatal germ cells as spermatogonial stem cells (8). In the present study, we have combined our NS-GFP-Tg system with a murine brain tumor model to investigate whether aggressive solid tumors contain a distinct population of T-ICs.

Results

High Frequency of Tumorigenic Cells in an Aggressive Murine Brain Tumor. T-ICs have been identified in human high-grade gliomas (glioblastoma multiforme), which are very aggressive, invasive, and

Author contributions: A.H. designed research; A.T., T.M., K.N., S.T., M.K., T.H., M. Ohmura, H. Shugo, and T.O. performed research; M. Onodera, K.M., and M.A. contributed new reagents/analytic tools; M.N., K.S., M. Oshima, H. Saya, H.O., T.S., J.-i.H., and A.H. analyzed data; and A.T. and A.H. wrote the paper.

The authors declare no conflict of interest.

This article is a PNAS Direct Submission.

[1]A.T., T.M., and K.N. contributed equally to this work.

[2]To whom correspondence should be addressed. E-mail: ahirao@kenroku.kanazawa-u.ac.jp.

This article contains supporting information online at www.pnas.org/cgi/content/full/0905016106/DCSupplemental.

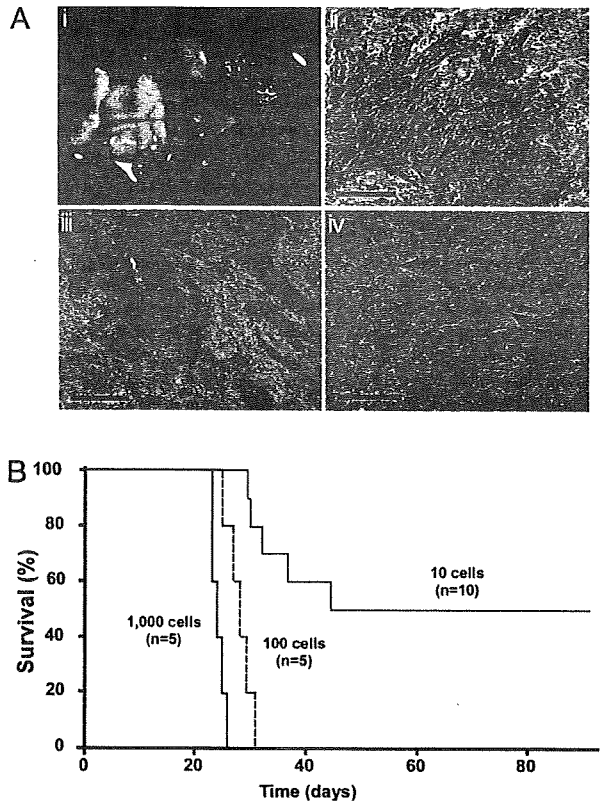

Fig. 1. High frequency of tumorigenic cells in a murine brain tumor. (*A*) Development of brain tumors. (*i*) Gross appearance of a recipient brain. A massive lesion can be seen in the cerebrum. (*ii–iv*) H&E staining of representative sections of brain tumors. Regions of increased cell density, nuclear pleomorphism, and prominent mitotic figures can be seen. Arrows, giant cells; arrowheads, areas of necrosis with pseudopalisading; asterisks, invading tumor cells adjacent to blood vessels. (Scale bars: 200 μm.) (*B*) Survival of recipient mice after transplantation of 1,000, 100, or 10 huKO$^+$ tumor cells, as indicated.

destructive brain tumors (12). Invasive tumor cells escape surgical removal and geographically dodge lethal radiation exposure and chemotherapy. A mouse brain tumor model of human glioblastoma multiforme can be generated by triggering Ras signaling downstream of the epidermal growth factor (EGF) receptor in brain cells of mice deficient for the tumor suppressors p16^{Ink4a}/p19^{Arf} (13–15). We modified the reported protocol (15) and constructed a vector containing a constitutively active mutant K-ras gene (K-ras^{G12V}) plus the humanized Kusabira-Orange (huKO) gene as a marker. We used retroviral infection to introduce this vector into cultured neurospheres composed of neural stem cells and precursor cells (NSC/NPCs) derived from the subventricular zone (SVZ) of brains of neonatal p16$^{Ink4a-/-}$/p19$^{Arf-/-}$ mice. The infected neurospheres were then injected into the basal ganglia of wild type (WT) recipient mice (Fig. S1). Brain tumors developed as early as 20 days after transplantation, and most recipients died within 40 days of injection. Consistent with previous reports (13–16), histological analyses of these tumors demonstrated that these tumors showed several features characteristic of human gliomas (17), including microvascular proliferation, the presence of giant cells, and/or areas of tumor necrosis bordered by dense palisades of viable tumor cells (necrosis with pseudopalisading) (Fig. 1*A*).

To analyze the frequency of T-ICs within tumors, the malignancies were recovered from recipients and dissociated by collagenase treatment. To eliminate any contaminating normal brain cells, flow cytometry was used to collect huKO$^+$ cells (i.e., cells overexpressing K-ras^{G12V}). Transplantation of 100 or 1,000 freshly isolated tumor cells into the brains of WT mice (8 weeks old) resulted in brain tumor formation in 100% of recipients (Fig. 1*B*). Even when only 10 tumor cells were injected, 50% of recipients developed brain tumors, suggesting that the frequency of tumorigenic cells in the original tumor was very high.

Correlation of In Vivo Differentiation Status of NSC/NPC and GFP Fluorescence Intensity in NS-GFP-Tg Brain. Tsai and McKay have reported that NS is highly expressed in undifferentiated NSC/NPCs but not in differentiating neurons (9). To determine whether the NS-GFP system marked NSC/NPCs, we evaluated GFP expression in embryonic brains of our NS-GFP-Tg mice. In embryonic brain at E14.5, radial glial cells in the ventricular zone are NSC/NPCs. At this stage, the cortical plate is formed by active neurogenesis derived from NSC/NPCs (18). In the NS-GFP-Tg brain at E14.5, higher GFP expression was observed in ventricular zone cells expressing nestin (19) or musashi-1 (20), a protein enriched in NSC/NPCs, whereas TuJ1$^+$ neurons showed a lower level of GFP (Fig. 2*A* and Fig. S2). In neonatal brain (P3), GFP was highly expressed in SVZ, which are actively cycling, and down-regulated in the striatum (Fig. S3). These analyses suggested that NSC/NPCs are included within the subpopulation of normal brain cells that expresses high levels of GFP.

To investigate the relationship between GFP fluorescence intensity and cellular properties, we used flow cytometry to divide the total cell population recovered from dissociated E14.5 NS-GFP-Tg brains into four fractions according to GFP fluorescence intensity: GFP$^{-/+}$, GFP^{++}, GFP^{+++} and GFP^{++++} (Fig. 2*B*). Immunostaining of the sorted cells with anti-nestin or anti-TuJ1 revealed that most GFP^{++++} cells expressed nestin but not TuJ1 (Fig. 2*C*), indicating that they were undifferentiated. In contrast, GFP$^{-/+}$ cells expressed TuJ1 but not nestin. Thus, our NS-GFP-Tg system allows us to monitor stem cell differentiation during neurogenesis. When we examined the capacity of our four GFP-expressing subpopulations to form neurospheres, we found that neurosphere-initiating cells were most efficiently generated by cells with higher GFP expression, whether these cells were derived from embryonic (E14.5) or neonatal (P3) NS-GFP-Tg brains (Fig. 2 *D–F*). In particular, half of the total neurosphere-initiating cells in neonatal brain were enriched in the rare (10%) GFP^{++++} cell population. Our findings support previous reports showing that neurosphere-initiating cells are enriched in sorted GFP-strong positive cells isolated from the brains of *nestin*-EGFP mice (21). We conclude that brain cells in our NS-GFP system that express very high levels of GFP exhibit a substantial capacity for both proliferation and NSC/NPC differentiation.

Identification of Brain T-ICs. Our success in monitoring normal NSC/NPC differentiation in NS-GFP-Tg mice prompted us to use this system to analyze cellular heterogeneity in our brain tumor model. We crossed our NS-GFP-Tg mice to p16$^{Ink4a-/-}$/p19$^{Arf-/-}$ mice and induced the generation of brain tumors as described above. Flow cytometric analyses of these huKO$^+$ tumors derived from NS-GFP-Tg mice revealed that they contained both GFP^{high} and GFP^{low} populations. The ratio of GFP^{high} to GFP^{low} cells was highly variable among individual tumors (Fig. 3*A*). Immunocytochemical analysis of freshly isolated tumor cells confirmed that endogenous NS was highly expressed in GFP^{high} cells but not in GFP^{low} cells (Fig. S4). CD133 (prominin 1) or nestin has been reported to be a marker of T-ICs in human glioma. The expression pattern of prominin 1 mRNA varied among tumors (Fig. S5); however, we found that GFP^{high} cells primarily expressed nestin, whereas the GFP^{low} population showed nestin down-regulation (Fig. 3*B*). These data suggested that the GFP^{high} tumor cells might be immature cells with the potential to differentiate into GFP^{low} tumor cells in vivo.

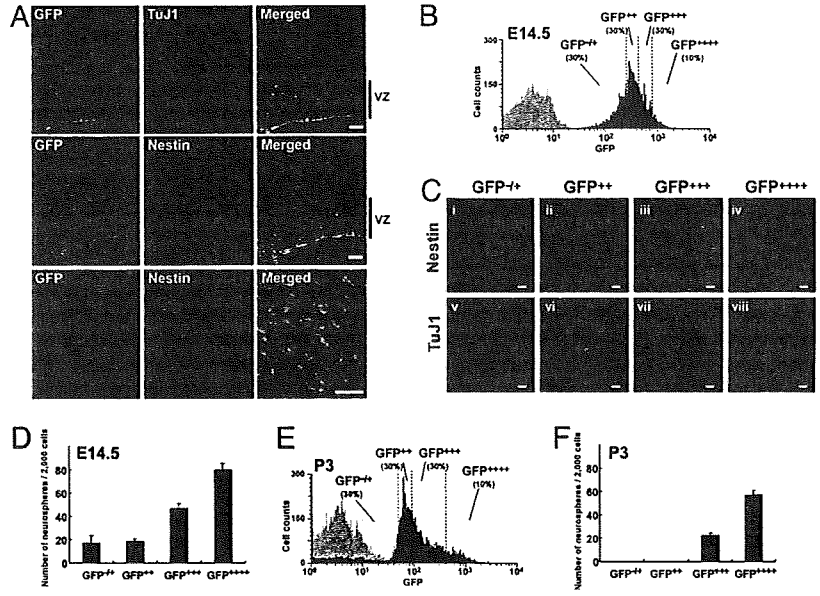

Fig. 2. Correlation of in vivo differentiation status of NSC/NPC and GFP fluorescence intensity in the NS-GFP-Tg brain. (*A*) High GFP expression correlates with high nestin expression in cells of NS-GFP-Tg embryonic forebrains. Coronal sections of forebrains of E14.5 NS-GFP-Tg mice were subjected to immunohistochemical analysis using anti-GFP (green) plus anti-type III β-tubulin (TuJ1; red, *Top*), or anti-GFP plus anti-nestin (red, *Middle* and *Bottom*). Images of the ventricular zone (VZ) cells in the *Middle* are shown at higher magnification in *Bottom*. (Scale bars: *Top* and *Middle*, 100 μm; *Bottom*, 10 μm). (*B*) Fractionation of GFP-expressing cells from E14.5 NS-GFP-Tg brain. Total brain cells from E14.5 NS-GFP-Tg mice were dissociated and fractionated by flow cytometry into 4 subpopulations, $GFP^{-/+}$, GFP^{++}, GFP^{+++} and GFP^{++++}, based on GFP fluorescence intensity as indicated. Gray peak, WT C57BL/6 mice; black peak, NS-GFP-Tg mice. (*C*) Correlation of high GFP expression with immature cell properties. The fractionated brain cell subpopulations from *B* were fixed and analyzed by immunocytochemistry to detect expression of nestin (red, *i–iv*) or TuJ1 (red, *v–viii*) as indicated. Blue, nuclear marker TOTO-3. (Scale bars, 20 μm.) (*D*) Correlation of GFP expression with neurosphere-forming capacity in E14.5 NS-GFP-Tg brain tissues. Fractionated brain cell subpopulations from *B* were cultured under conditions allowing neurosphere formation. Data shown are the mean number ± SD. of neurospheres generated per 2,000 cells (n = 3 per group). (*E*) Fractionation of P3 GFP-expressing brain cells. Total brain cells from P3 NS-GFP-Tg mice were dissociated and fractionated by flow cytometry into 4 subpopulations, $GFP^{-/+}$, GFP^{++}, GFP^{+++} and GFP^{++++}, based on GFP fluorescence intensity as indicated. Gray peak, WT C57BL/6 mice; black peak, NS-GFP-Tg mice. (*F*) Correlation of GFP expression with neurosphere-forming capacity in P3 NS-GFP-Tg brain tissues. The fractionated brain cell subpopulations in *E* were cultured to allow neurosphere formation as for *D*. Data shown are the mean number ± SD. of neurospheres generated per 2,000 cells (n = 3 per group).

To investigate the properties of the GFP^{high} and GFP^{low} tumor cells, we first evaluated their capacity to form spheres in culture. Many spheres were generated in cultures of GFP^{high} cells, whereas GFP^{low} cells produced only a few spheres (Fig. 3*C*). To investigate the behavior of the GFP^{high} and GFP^{low} tumor cells in vivo, the cells were orthotopically transplanted into WT mice to generate new brain tumors. All mice receiving 10,000 GFP^{high} cells developed brain tumors (Fig. 3*D*). However, the frequency of tumorigenicity was decreased and tumor onset was delayed in mice that received 10,000 GFP^{low} tumor cells. Because it was possible that the GFP^{low} cell population had been contaminated by a very small number of GFP^{high} cells, the transplant cell number was reduced to eliminate the possibility of contamination. No tumor arose in recipients even when 1,000 GFP^{low} cells were transplanted, but injection of 1,000 or 100 GFP^{high} cells was sufficient to generate brain tumors in 100% of recipients. When only 10 tumor cells were injected, 60% of recipients developed brain tumors. Thus, our NS-GFP system significantly distinguishes tumorigenic from nontumorigenic cells.

We next explored the cellular heterogeneity of tumors developing in WT recipient brains. Histological analysis showed that malignancies developing in WT mice that had received 10 GFP^{high} tumor cells tended to show less morphological variability than the original brain tumors (Fig. 3*E*), suggesting that the latter may have arisen from multiple clones with different retrovirus integration sites. Nonetheless, the pattern of GFP expression in cells of the transplanted tumors was similar to that in the original tumors, in that secondary tumors also had both GFP^{high} and GFP^{low} populations (Fig. 3*E*). Because the brain tumors generated by injection of 10 GFP^{high} tumor cells were not necessarily of single-cell origin, we performed limiting dilution experiments on the original tumors to isolate single cell-derived tumors. All neurospheres derived from such single tumor cells exhibited bright GFP fluorescence (Fig. 3*F*). When such GFP^{bright} neurospheres were injected into WT recipient mice, the resulting brain tumors also contained GFP^{high} and GFP^{low} tumor cells and therefore recapitulated the original GFP expression pattern (Fig. 3*G*). These clonal studies conclusively establish that bona fide functional heterogeneity can exist among cells comprising a genetically homogeneous tumor, and T-ICs can be identified in highly aggressive tumors.

Invasiveness of T-ICs. To better understand T-IC behavior, we used our NS-GFP-Tg brain tumor model to track the localization of GFP^{high} tumor cells in vivo. Immunohistochemical analyses of sections of either the single-cell-derived tumors or the original tumors showed the tumor cells expressing GFP (GFP^+ cells) were localized predominantly in the areas of the tumor facing normal tissues (Fig. 4 *A*, *B*, and *D*), whereas tumor cells located in center of the malignancy did not express GFP (Fig. 4*C* and Fig. S6). Scattered GFP^+ tumor cells also invaded the normal brain tissue adjacent to the tumor (Fig. 4 *B* and *D*). A typical feature of human gliomas is the spreading of tumor cells along the basement membranes of blood vessels. As shown in Fig. 4 *E* and *F*, blood vessels adjacent to the tumor were surrounded by GFP^+ cells, suggesting that these T-ICs drive the invasion of the malignancy into normal brain tissues.

We next compared GFP^{high} and GFP^{low} cells from brain tumors for expression of genes responsible for tumor cell migration and invasion. We found that c-Met, a receptor tyrosine kinase that binds hepatocyte growth factor (HGF), was expressed at much higher levels in the GFP^{high} cells of a given tumor than in the tumor's GFP^{low} cells (Fig. 5*A*). HGF, originally identified as a mitogen for hepatocytes, potently enhances dissociation of cell–cell adhesiveness, cell motility, and extracellular matrix breakdown, thereby promoting tumor cell invasion and metastasis (22, 23). Several studies suggest that inhibition of the HGF/c-Met pathway is of therapeutic benefit in cases of human glioma (24–26). When we carried out immunohistochemical analyses of our brain tumors, we found that c-Met was phosphorylated in GFP^+ tumor cells at the invasion front of the malignancy (Fig. 5*B*), indicating that the T-ICs showed activation of c-Met signal. To analyze whether these T-ICs indeed have potential for migration in response to c-Met/HGF signaling, we inoculated tumor cells into a collagen gel containing HGF. Although HGF did not affect number of sphere formation, it dramatically induced the migration and elongation of GFP^+

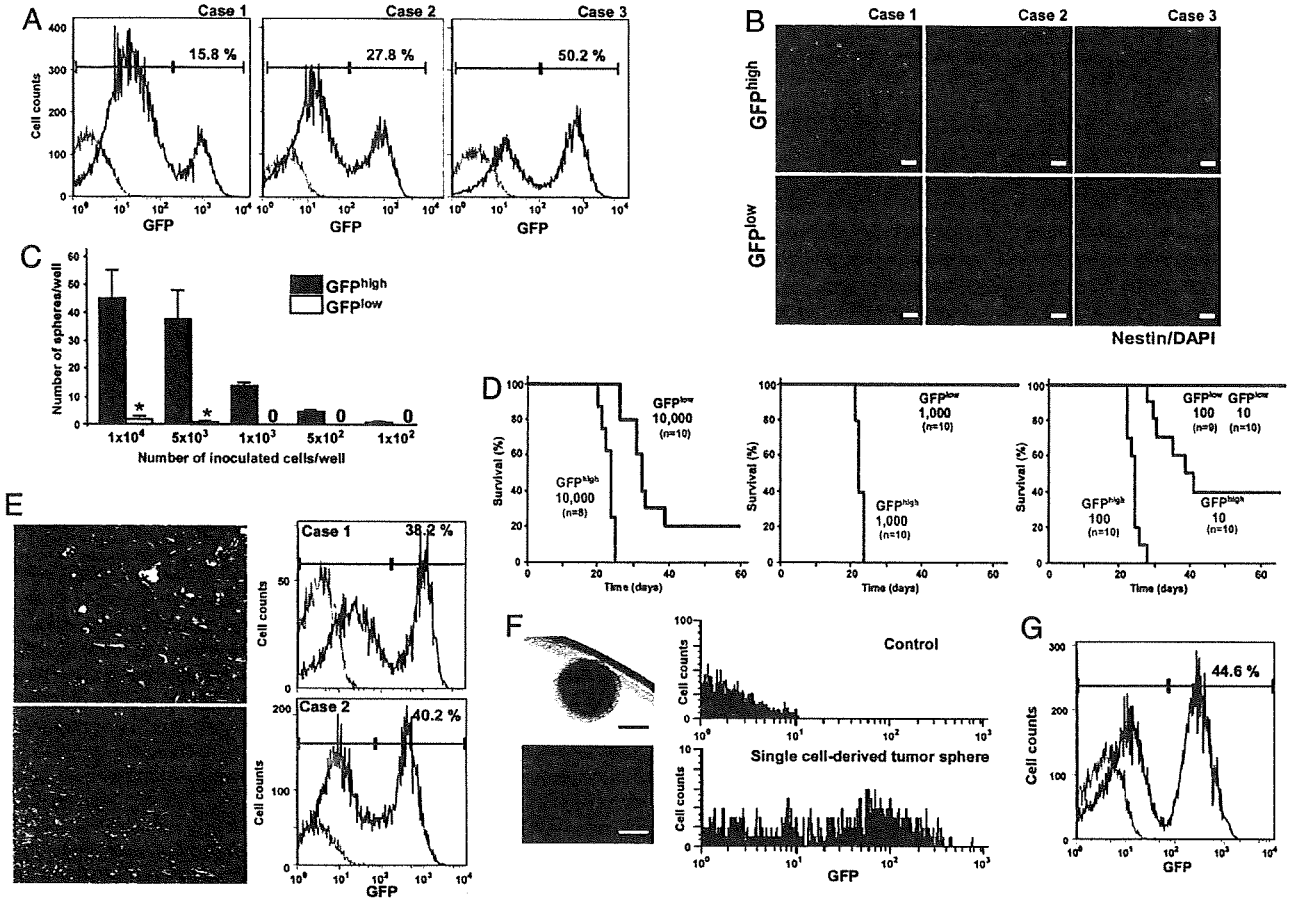

Fig. 3. Identification of T-ICs. (*A*) Detection of GFP^{high} and GFP^{low} subpopulations among brain tumor cells derived from NS-GFP-Tg mice. Tumors were dissociated with collagenase and GFP expression was analyzed in huKO^{+} tumor cells by flow cytometry. Tumors contained variable percentages of GFP^{high} and GFP^{low} cells. Three representative samples showing the GFP expression pattern in huKO^{+} tumor cells are shown. (*B*) GFP^{high} tumor cells exhibit immature cell properties. Cytospin smears of sorted GFP^{high} and GFP^{low} cells in *A* were fixed and immunostained to detect nestin (red). Blue, nuclear marker DAPI. Three representative samples of 5 independent experiments are shown. (Scale bars: 20 μm.) (*C*) GFP^{high} tumor cells can generate spheres. GFP^{high} and GFP^{low} cells from brain tumors in *A* were cultured for 14 days under sphere formation conditions. Data shown are the mean number ± SD. of spheres per indicated number of inoculated cells (n = 4 per group; *, $P < 0.01$). (*D*) Transplantation of GFP^{high} brain tumor cells curtails survival. The percentage survival of WT recipient mice injected with 10,000, 1,000, 100, or 10 GFP^{high} or GFP^{low} brain tumor cells is shown as indicated. (*E*) Maintenance of the GFP expression pattern between original and transplanted brain tumors. Analysis of histology (by H&E staining, *Left*) and GFP expression (by flow cytometry, *Right*) of brain tumors isolated from two WT recipient mice transplanted with 10 GFP^{high} brain tumor cells (as from *D*, *Right*). (Scale bars: 200 μm.) (*F*) A neurosphere derived from a single tumor cell by limiting dilution. (*Left Upper*) Bright field. (*Left Lower*) GFP fluorescence. (Scale bars: 200 μm.) *Right*, GFP fluorescence as determined by flow cytometry. (*Upper*) Neurospheres from control mice (P3). (*Lower*) Single cell-derived spheres from NS-GFP tumor. Representative data are shown. (*G*) Maintenance of GFP expression pattern between original tumors and tumors arising from transplantation of single-cell-derived neurospheres. Neurospheres derived in culture from single cells of an original tumor were transplanted into WT recipient mice. Tumors arising in these recipients were dissociated and the expression of their component cells analyzed. Data representative of 4 independent experiments are shown.

T-ICs placed in a collagen gel (Fig. 5*C*). These T-ICs therefore have the potential to respond to HGF and migrate through a matrix with collagenase activity. These data suggest that the T-ICs identified by our NS-GFP-Tg system lead the invasion of the malignancy into normal brain tissue.

Discussion

In this study, we used a murine brain tumor model to establish that even in aggressive brain tumors that contain a high frequency of T-ICs, T-ICs represent a distinct cell type capable of generating non-T-ICs, which comprise the bulk of the tumor tissue. The use of a syngenic and orthotopic system overcomes limitations of xenotransplant systems, which typically show relatively low frequencies of T-ICs in human brain tumors (5). The concern that environmental differences existing between human and mouse tissues might lead to an underestimation of tumorigenic cell frequency may be supported by our data. It could be argued that our tumor model is more aggressive than a spontaneous tumor because we generate malignancies by oncogene overexpression. However, although the tumors were generated experimentally, histological analyses demonstrate that these tumors exhibit apparent heterogeneity, similar to human gliomas. Our results clearly demonstrate that, if the appropriate marker is available, T-ICs can be identified in an aggressive solid tumor regardless of their frequency.

Optimization of xenotransplantation assays by using highly immunocompromised NOD/SCID/Il2r$\gamma^{-/-}$ mice dramatically improved the transplantation efficiency of human melanoma cells, compared with traditional NOD/SCID mice (7), suggesting that the human melanoma randomly form tumor in the mice or genetic heterogeneity might be related to ability to form tumors, but not due to hierarchical organization. However, examinations of human acute myeloid leukemia (AML) have demonstrated that L-ICs are

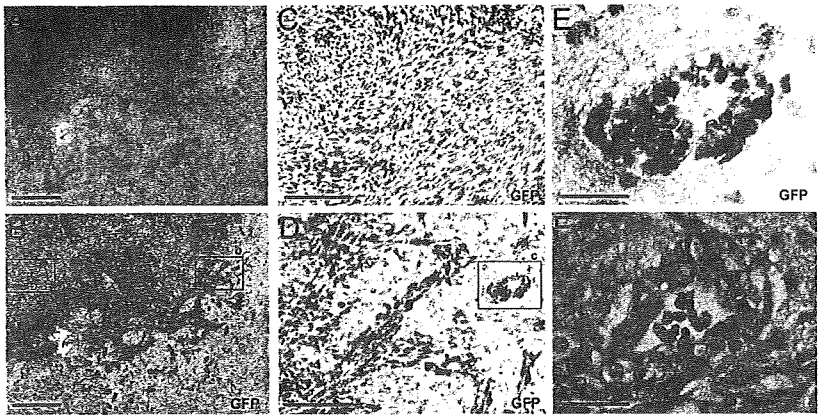

Fig. 4. Localization of T-ICs. Serial sections of a single-cell-derived tumor were stained with H&E (*A* and *F*) or anti-GFP (*B–E*) to identify T-ICs. (*A*) H&E staining of a tumor invading normal brain tissue. (*B*) Anti-GFP staining of the tissue in *A*. (*a* and *b*) Low-power views of areas shown at high power in *C* and *D*, respectively. (*E*) High-power view of area *c* in *D*. (*F*) H&E staining of *E*. (Scale bars: *A* and *B*, 1 mm; *C* and *D*, 200 μm; *E* and *F*, 50 μm.)

rare even when analyzed in NOD/SCID/Il2rγ$^{-/-}$ mice (27). A recent study of syngenic transplantation using mouse mammary tumor models also identified relatively rare T-ICs (28), suggesting that the frequencies of T-ICs may depend on type of cancer. Indeed, in our study, the frequency of GFP^{high} T-ICs varied greatly among individual brain tumors. In the case of a malignancy with a very high frequency of T-ICs (e.g., Fig. 3*A*, case 3), we surmise that most of the brain tumor cells present were "CSCs," as occurs in human melanomas. In other cases (e.g., Fig. 3*A*, case 1), the percentage of T-ICs was relatively low. Although we cannot yet be sure precisely what factors determine the frequency of T-ICs in a given tumor, we suspect that the stage of cancer progression (e.g., early versus late stage) is also important. Furthermore, we assume that the cell cycle status of T-ICs may also vary depending on the nature of the tumor. It has been previously reported that human leukemias include rare L-ICs, which showed slow cycling (27). In contrast, the GFP^{high} T-ICs in brain tumors analyzed in this study were actively cycling (Fig. S7). We hypothesize that, in the case of tumors showing a high frequency of T-ICs like our brain tumor model or human melanoma, T-ICs are actively cycling, resulting in very aggressive tumors.

Our NS-GFP-Tg system has allowed us to identify normal stem/progenitor cell populations in several different mouse tissues, including those responsible for neurogenesis and spermatogenesis (8). Although the population of cells strongly expressing GFP in each NS-GFP-Tg tissue may include progenitors, not only stem cells, we have observed a consistent relationship between GFP fluorescence intensity and degree of cellular maturation that has held across tissues. In addition, we also found that brain T-ICs were enriched by the NS-GFP system. Thus, both normal and tumor cells may use the same "stemness" programs. To investigate whether the NS-GFP system identify the "stemness" programs in tumor cell lines, we transfected the C6 glioma cell line with the NS-GFP construct and established stable clones. Although we found that most NS-GFP C6 cells in a single clone expressed GFP, as was the case in NS-GFP E14.5 embryonic brain, we did not observe differences in colony forming ability among subpopulations in C6 cells (Fig. S8). The inability to distinguish C6 T-ICs based on the NS-GFP expression is possibly due to that the fact that cultured C6 cells are more homogeneous than tumor tissue in vivo.

A key characteristic of human gliomas is their ability to invade normal brain tissue. As shown in Fig. 4, some tumor cells adjacent to blood vessels may lose GFP, suggesting that NS-GFP^{high} T-ICs may not be the only cells responsible for tumor invasion. However, we do not believe that NS-GFP^{low} cells adjacent to blood vessels contribute to tumor progression or expansion, because they lose the capacity for tumor-initiation, as shown in Fig. 3*D*. Glioma invasiveness is of clinical relevance, because brain tumor recurrence occurs most often within the surgical resection margin (12). Therefore, we believe that NS-GFP^{high} cells are primarily responsible for in invasion. The use of our stem cell concept-based system to further investigate tumor organization may increase our understanding of the nature of cancer and lead to the development of novel cancer therapies.

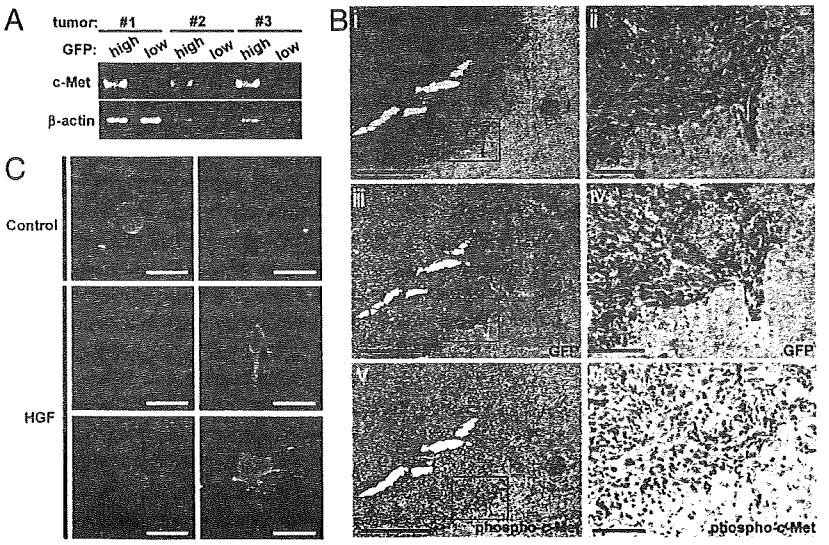

Fig. 5. Migration potential of T-ICs. (*A*) High expression of c-Met in GFP^{high} cells. Total RNA was purified from GFP^{high} and GFP^{low} cells isolated from three independent original tumors and c-Met mRNA levels were evaluated by RT-PCR. β-actin, control. (*B*) c-Met is phosphorylated in T-ICs. Serial sections of one of the single cell-derived tumors were subjected to H&E (*i* and *ii*); anti-GFP (*iii* and *iv*); and anti-phospho-c-Met (*v* and *vi*) staining. Magnified views of the areas indicated by the squares in *i*, *iii* and *v* are shown in *ii*, *iv*, and *vi*, respectively. (Scale bars: *i*, *iii*, *v*, 1 mm; *ii*, *iv*, *vi*, 200 μm.) (*C*) Migration of T-ICs in a collagen gel. Dissociated cells from a tumor were inoculated into either a plain collagen gel (control) or a collagen gel containing HGF (10 ng/mL) and incubated for 4 days. Representative GFP^{+} tumor cells with and without HGF in a collagen gel are shown. (Scale bars: 50 μm.)

Methods

Mice. All data presented in this study were obtained from experiments using heterozygous NS-GFP-Tg mice as described in ref. 8. $p16^{Ink4a+/-}/p19^{Arf+/-}$ mice were obtained from the Mouse Models of Human Cancers Consortium (MMHCC), National Cancer Institute-Frederick (29). All mice are of the C57BL/6 background. All animal procedures were performed in accordance with the animal care guidelines of Kanazawa University.

Generation of the Brain Tumor Model. A mutant K-ras^{G12V} gene was cloned into the retroviral vector pGCDN sap IRES huKO (30). Using Plat-E with *Lipofectin* Reagent (Invitrogen) (31), this vector was transfected into cells from the subventricular zone of NS-GFP-Tg/$p16^{Ink4a-/-}/p19^{Arf-/-}$ neonates (P4–5) that had been maintained under neurosphere culture conditions for 7days. The infected neurosphere cells were transplanted into the basal ganglia of 8–10-week-old C57BL/6 mice to generate brain tumors containing NS-GFP-Tg tumor cells.

Sphere Formation. Brain tumor cells or normal cells isolated from the brains of NS-GFP-Tg embryos or neonates and fractionated according to GFP fluorescence intensity. Cells from each fraction (1×10^3 cells per 100 μL) were cultured as described in ref. 32 in DMEM/F12-based serum-free growth medium containing insulin (25 μg/mL), transferrin (100 μg/mL), progesterone (20 nM), sodium selenate (30 nM), EGF (20 ng/mL), and bFGF (20 ng/mL). All reagents were from Sigma except for EGF, which was obtained from Stem Cell Technologies. On day 7 or 14, the number of spheres of diameter >50 μm was counted under a phase-contrast microscope.

Immunohistochemistry. Tumor or normal embryonic brain tissues were fixed in 4% paraformaldehyde and sections were immunostained with the following primary antibodies: mouse anti-nestin (BD), mouse anti-type III β-tubulin (TuJ1, Sigma), goat-anti-nucleostemin (R&D Systems), rabbit-anit-nucleostemin (Novus), rabbit-anti-GFP (Invitrogen), rabbit-anti-GFAP (Dakocytomation), and rabbit-anti-phosphorylated c-Met (Invitrogen). The staining signals for paraffin-embedded sections were visualized with peroxidase-conjugated secondary antibody (Amersham Biosciences), and counterstained with hematoxylin using the DAB Peroxidase Substrate Kit (VECTOR). The staining signals for frozen sections were visualized with the Alexa Fluor dye-conjugated secondary antibody: anti-mouse IgG, anti-rabbit IgG, or anti-goat IgG (Molecular Probes). Completed immunostaining was visualized using confocal microscopy (Olympus FV1000). For immunocytochemistry, cells were collected by flow cytometry and cytospin smears were prepared. Immunostaining was visualized using confocal microscopy. For visualization of nuclei, specimens were stained with DAPI or TOTO-3 (Molecular Probes).

Flow Cytometry. Tumor tissues were dissociated with 1 mg/mL collagenase (Sigma), whereas normal brain tissues were dissociated using a pipetting procedure. Cell sorting and flow cytometric analyses were performed using JSAN (Bay Bioscience). Sorted cells were resuspended in DMEM containing 10% FBS, washed once with medium, and prepared for further analysis. For transplantation or sphere formation experiments, we sorted subpopulations twice by flow cytometry. For some experiments, cytospin smears of the sorted cells were fixed with 4% paraformaldehyde.

Collagen Gel Invasiveness Assay. Freshly isolated tumor cells were suspended at 1×10^3 cells in 40 μL of ice-cold neutralized collagen type I from rat tail (2.4 mg/mL; BD) and incubated at 37 °C for 30 min. The resulting cell aggregates were further embedded in 500 μL of collagen type I solution (2.4 mg/mL) and solidified. The gels were floated on 500 μL of sphere formation medium containing EGF (20 ng/mL) and bFGF (20 ng/mL), with or without human recombinant HGF (10 ng/mL). This HGF was purifed from the conditioned medium of Chinese hamster ovary cells transfected with human HGF cDNA (22). The purity of the HGF was >98% as determined by SDS/PAGE and protein staining.

RT-PCR Analysis. RNA samples were purified from fractionated tumor cells (1×10^5) using the RNeasy kit (QIAGEN) and reverse-transcribed using the Advantage RT-for-PCR kit (Clontech). PCR was performed using a GeneAmp PCR system 9,700 (PE Applied Biosystems). The following primers were used: 5′-AGCATTTCTC-CGAGGTACGG-3′ and 5′-CATTGAGATCATTACTGGCT-3′ for c-Met; 5′-GTACCT-CAGATCCAGCCAGCAA-3′ and 5′-ATTCTTCCAGCTTGGGCAGC-3′ for prominin 1; 5′-AGGTCATCACTATTGGCAACGA-3′ and 5′-CACTTCATGATGGAATTGAATG-TAGTT-3′ for β-actin.

Statistical Analyses. *P* values were calculated using the unpaired Student's *t* test.

ACKNOWLEDGMENTS. We thank Dr. John E. Dick for helpful suggestions and critical reading of the manuscript, Miyako Takegami and Akiko Imamura for technical assistance, Dr. Toshio Kitamura for providing Plat-E, and Dr. Yoshinori Suzuki for help on the collagen gel invasiveness assay. This work was supported by Ministry of Education, Culture, Sports, Science and Technology, Japan Grant-in-Aid for Scientific Research on Priority Areas and Creative Scientific Research and for Cancer Research 17GS0419 (to A.H.) and a grant from the Ministry of Health, Labour and Welfare, Japan, for the Third-Term Comprehensive 10-year Strategy for Cancer Control (to A.H.) and in part by Kyowa Hakko Kirin Co. Ltd.

1. Pardal R, Clarke MF, Morrison SJ (2003) Applying the principles of stem-cell biology to cancer. *Nat Rev Cancer* 3:895–902.
2. Dick JE (2009) Looking ahead in cancer stem cell research. *Nat Biotechnol* 27:44–46.
3. Barabe F, Kennedy JA, Hope KJ, Dick JE (2007) Modeling the initiation and progression of human acute leukemia in mice. *Science* 316:600–604.
4. Al-Hajj M, Wicha MS, Benito-Hernandez A, Morrison SJ, Clarke MF (2003) Prospective identification of tumorigenic breast cancer cells. *Proc Natl Acad Sci USA* 100:3983–3988.
5. Singh SK, et al. (2004) Identification of human brain tumour initiating cells. *Nature* 432:396–401.
6. Schatton T, et al. (2008) Identification of cells initiating human melanomas. *Nature* 451:345–349.
7. Quintana E, et al. (2008) Efficient tumour formation by single human melanoma cells. *Nature* 456:593–598.
8. Ohmura M, et al. (2008) Identification of stem cells during prepubertal spermatogenesis via monitoring of nucleostemin promoter activity. *Stem Cells* 26:3237–3246.
9. Tsai RY, McKay RD (2002) A nucleolar mechanism controlling cell proliferation in stem cells and cancer cells. *Genes Dev* 16:2991–3003.
10. Beekman C, et al. (2006) Evolutionarily conserved role of nucleostemin: Controlling proliferation of stem/progenitor cells during early vertebrate development. *Mol Cell Biol* 26:9291–9301.
11. Maki N, et al. (2007) Rapid accumulation of nucleostemin in nucleolus during newt regeneration. *Dev Dyn* 236:941–950.
12. Nakada M, et al. (2007) Molecular targets of glioma invasion. *Cell Mol Life Sci* 64:458–478.
13. Holland EC, et al. (2000) Combined activation of Ras and Akt in neural progenitors induces glioblastoma formation in mice. *Nat Genet* 25:55–57.
14. Uhrbom L, et al. (2002) Ink4a-Arf loss cooperates with KRas activation in astrocytes and neural progenitors to generate glioblastomas of various morphologies depending on activated Akt. *Cancer Res* 62:5551–5558.
15. Bachoo RM, et al. (2002) Epidermal growth factor receptor and Ink4a/Arf: Convergent mechanisms governing terminal differentiation and transformation along the neural stem cell to astrocyte axis. *Cancer Cell* 1:269–277.
16. Marumoto T, et al. (2009) Development of a novel mouse glioma model using lentiviral vectors. *Nat Med* 15:110–116.
17. Louis DN, et al. (2007) The 2007 WHO classification of tumours of the central nervous system. *Acta Neuropathol* 114:97–109.
18. Merkle FT, Alvarez-Buylla A (2006) Neural stem cells in mammalian development. *Curr Opin Cell Biol* 18:704–709.
19. Lendahl U, Zimmerman LB, McKay RD (1990) CNS stem cells express a new class of intermediate filament protein. *Cell* 60:585–595.
20. Sakakibara S, et al. (1996) Mouse-Musashi-1, a neural RNA-binding protein highly enriched in the mammalian CNS stem cell. *Dev Biol* 176:230–242.
21. Kawaguchi A, et al. (2001) Nestin-EGFP transgenic mice: Visualization of the self-renewal and multipotency of CNS stem cells. *Mol Cell Neurosci* 17:259–273.
22. Nakamura T, et al. (1989) Molecular cloning and expression of human hepatocyte growth factor. *Nature* 342:440–443.
23. Matsumoto K, Nakamura T (2006) Hepatocyte growth factor and the Met system as a mediator of tumor-stromal interactions. *Int J Cancer* 119:477–483.
24. Brockmann MA, et al. (2003) Inhibition of intracerebral glioblastoma growth by local treatment with the scatter factor/hepatocyte growth factor-antagonist NK4. *Clin Cancer Res* 9:4578–4585.
25. Martens T, et al. (2006) A novel one-armed anti-c-Met antibody inhibits glioblastoma growth in vivo. *Clin Cancer Res* 12:6144–6152.
26. Tseng JR, et al. (2008) Preclinical efficacy of the c-Met inhibitor CE-355621 in a U87 MG mouse xenograft model evaluated by 18F-FDG small-animal PET. *J Nucl Med* 49:129–134.
27. Ishikawa F, et al. (2007) Chemotherapy-resistant human AML stem cells home to and engraft within the bone-marrow endosteal region. *Nat Biotechnol* 25:1315–1321.
28. Vaillant F, et al. (2008) The mammary progenitor marker CD61/beta3 integrin identifies cancer stem cells in mouse models of mammary tumorigenesis. *Cancer Res* 68:7711–7717.
29. Serrano M, et al. (1996) Role of the INK4a locus in tumor suppression and cell mortality. *Cell* 85:27–37.
30. Sanuki S, et al. (2008) A new red fluorescent protein that allows efficient marking of murine hematopoietic stem cells. *J Gene Med* 10:965–971.
31. Morita S, Kojima T, Kitamura T (2000) Plat-E: An efficient and stable system for transient packaging of retroviruses. *Gene Ther* 7:1063–1066.
32. Reynolds BA, Weiss S (1996) Clonal and population analyses demonstrate that an EGF-responsive mammalian embryonic CNS precursor is a stem cell. *Dev Biol* 175:1–13.

Brief report

Definitive proof for direct reprogramming of hematopoietic cells to pluripotency

*Motohito Okabe,[1] *Makoto Otsu,[1] Dong Hyuck Ahn,[1] Toshihiro Kobayashi,[1] Yohei Morita,[1] Yukiko Wakiyama,[2] Masafumi Onodera,[3] Koji Eto,[1] Hideo Ema,[1] and Hiromitsu Nakauchi[1,2]

[1]Division of Stem Cell Therapy, Center for Stem Cell and Regenerative Medicine, Institute of Medical Science, University of Tokyo, Tokyo; [2]Japan Science and Technology Agency, Exploratory Research for Advanced Technology, Nakauchi Stem Cell and Organ Regeneration Project, Tokyo; and [3]Department of Genetics, National Research Institute for Child Health and Development, Tokyo, Japan

Generation of induced pluripotent stem cells (iPSCs) generally uses fibroblastic cells, but other cell sources may prove useful in both research and clinical settings. Although proof of cellular origin requires genetic-marker identification in both target cells and established iPSCs, somatic cells other than mature lymphocytes mostly lack such markers. Here we show definitive proof of direct reprogramming of murine hematopoietic cells with no rearranged genes. Using iPSC factor transduction, we successfully derived iPSCs from bone marrow progenitor cells obtained from a mouse whose hematopoiesis was reconstituted from a single congenic hematopoietic stem cell. Established clones were demonstrated to be genetically identical to the transplanted single hematopoietic stem cell, thus proving their cellular origin. These hematopoietic cell–derived iPSCs showed typical characteristics of iPSCs, including the ability to contribute to chimerism in mice. These results will prompt further use of hematopoietic cells for iPSC generation while enabling definitive studies to test how cellular sources influence characteristics of descendant iPSCs. (Blood. 2009; 114:1764-1767)

Introduction

Development of induced pluripotent stem cell (iPSC) technology has enabled generation of disease-specific pluripotent stem cells from the patient.[1] A typical method uses virus-mediated transfer of defined factors into fibroblastic cells[2-4] or marrow-derived mesenchymal cells.[1,5] Some other tissues are also reported as sources for iPSC generation, including murine hepatocytes and gastric epithelial cells,[6] human keratinocytes,[7] and very recently, human blood.[8] As the variability of cellular sources becomes greater, it is attractive to address an interesting question: is each iPSC clone derived from distinct sources unique in its characteristics? Although definitive proof of iPSC cellular origin requires genetic markers, as most somatic cells (except mature lymphocytes) lack such markers, no formal data have shown reprogramming of hematopoietic cells, aside from one study that used immunoglobulin genes as markers.[9] Here, we demonstrate definitive proof for a direct reprogramming to pluripotency of primary marrow hematopoietic cells with no gene rearrangement.

Methods

Mice

Animal experiments were performed with approval of the Institutional Animal Care and Use Committee of the Institute of Medical Science, University of Tokyo.

Generation of iPSCs from murine bone marrow progenitor cells

Lineage marker–negative (Lin^-) c-Kit^+ (Kit^+) cells were enriched using immunomagnetic beads. pMXs vectors[10] encoding iPSC genes are described.[1] Concentrated vesicular stomatitis virus-G–retroviral supernatant was prepared using reported procedures.[11-13] 293GP and 293GPG cells were kind gifts from Dr R. C. Mulligan (Children's Hospital Boston, Harvard Medical School, Boston, MA).[14] Detailed procedures are described in the text and supplemental data (available on the *Blood* website; see the Supplemental Materials link at the top of the online article).

In vitro and in vivo assessment of iPSCs

Characteristics of iPSCs were assessed following reported procedures.[1] Primer sequences are shown in supplemental Table 1. Immunoglobulin heavy chain gene rearrangement was analyzed following described methods.[15,16] A single-base difference within *Cd45* exon 25 was analyzed as reported.[17]

Results and discussion

To prove the cellular origin of iPSC clones formally, use of definitive genetic markers is necessary, as with reported reprogramming of mature B cells[9] and pancreatic beta cells.[18] Even if iPSCs are generated from hematopoietic stem/progenitor cells (HSPCs), nearly 100% positive for the hematopoietic marker CD45, one might argue, in light of reported generation of iPSCs from marrow stromal cells,[1,5] that a small number of nonhematopoietic cells had been reprogrammed. However, no such suitable marker exists for hematopoietic cells (excepting rearranged immunoreceptor genes in mature lymphocytes). We therefore exploited a prominent characteristic of the hematopoietic system: transplantation of a single hematopoietic stem cell (HSC) can reconstitute host hematopoiesis.[19]

Submitted February 4, 2009; accepted May 11, 2009. Prepublished online as *Blood* First Edition paper, June 29, 2009; DOI 10.1182/blood-2009-02-203695.

*M. Okabe and M. Otsu contributed equally to this work.

The online version of this article contains a data supplement.

The publication costs of this article were defrayed in part by page charge payment. Therefore, and solely to indicate this fact, this article is hereby marked "advertisement" in accordance with 18 USC section 1734.

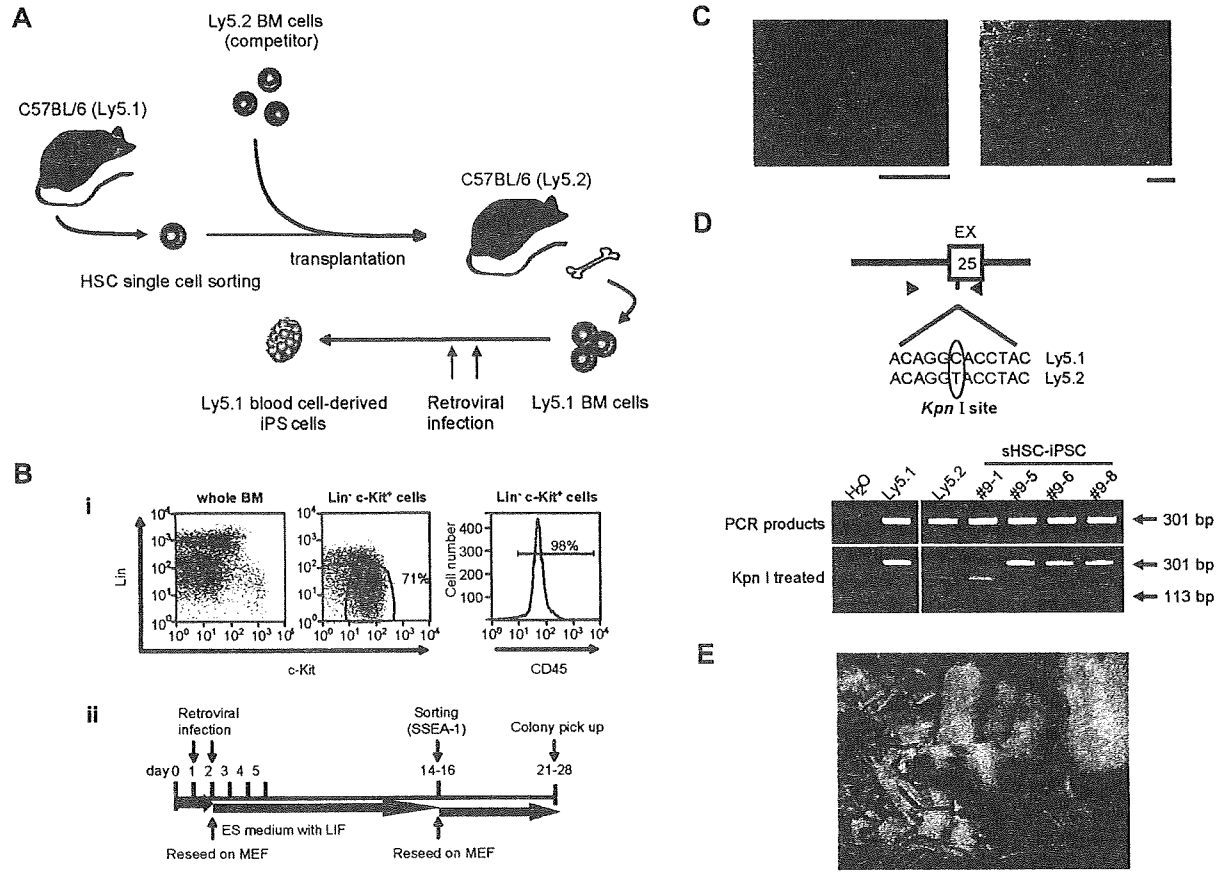

Figure 1. Proof of iPSC induction from hematopoietic cells in a single-HSC transplantation model. (A) Schematic representation of the experimental procedure. Single $CD150^+CD34^{-/low}$ KSL cells obtained from B6 Ly5.1 mice were transplanted into lethally irradiated B6 Ly5.2 mice together with BM cells from B6 Ly5.2 mice. BM HSPCs were obtained from a recipient mouse that showed long-term (~ 10 months) stable Ly5.1 chimerism (~ 80%), enriched for $Ly5.1^+$ cells, and subjected to iPSC generation. (B) A schematic diagram of iPSC generation from BM HSPCs. (i) Lineage markers (Lin) versus c-Kit plots are shown for cells either before (whole BM) or after ($Lin^-c\text{-}Kit^+$) purification. Note that purified HSPCs are 98% CD45-positive. (ii) A schematic diagram of iPSC generation from BM HSPCs. (C) Typical ES cell–like appearance of sHSC-iPS cell colonies (left) with high ALP activities (right). Bars represent 100 μm. (D) Determination of the cellular origin of sHSC-iPSC clones. (Top panel) Scheme of the polymerase chain reaction (PCR)–based method used, using a single-base polymorphism at *Cd45* exon (EX) 25. Black triangles represent primer positions. Ly5.1 and Ly5.2 strains differ by a single base in EX 25, as shown in the presented 12-bp sequences from within the 301-bp amplicons. Treatment with the restriction enzyme *Kpn*I leaves the $Ly5.1^+$ cell–derived amplicon undigested, whereas it generates 2 smaller fragments (113 bp + 188 bp) from the $Ly5.2^+$ counterpart. The gel images (bottom panel) indicate that, of 4 sHSC-iPSC clones, 1 (no. 9-1) is of $Ly5.2^+$ cell origin, whereas 3 (nos. 9-5, -6, and -8) are derived from $Ly5.1^+$ cells that originated from a single $Ly5.1^+$ HSC. A vertical line has been inserted to indicate a repositioned gel lane. (E) Chimeric mice obtained by implantation of sHSC-iPSC clone 9-5 into ICR host blastocysts.

Figure 1A depicts our experimental design. We attempted iPSC generation from marrow HSPCs harvested long-term (~ 10 months) after reconstitution from a single HSC of C57BL6 (B6) Ly 5.1 origin. We used concentrated vesicular stomatitis virus-G–pseudotyped retroviruses,[14] as we had succeeded in their efficient transduction into murine HSPCs.[12,13] We purified from bone marrow (BM) of a reconstituted mouse (B6 Ly5.2) Lin^-Kit^+ cells, a HSPC population, with approximately 98% of cells expressing CD45 (Figure 1B). We then transduced these cells with a cocktail of retroviral vectors harboring each of the iPSC factor genes *Oct4*, *Sox2*, *Klf4*, and *c-Myc*, transferred onto mouse embryonic fibroblast cells, and maintained in the presence of leukemia inhibitory factor until cell sorting (Figure 1B). Visible iPSC-like colonies appeared on approximately days 9 to 11 among a majority of hematopoietic cells that remained nonreprogrammed; these colonies then grew steadily (supplemental Figure 1A). To enrich iPSC candidates, we sorted the cells expressing SSEA-1 on approximately days 14 to 16 and allowed them to regrow for another 7 to 12 days (Figure 1B). Generated iPSC-like colonies showing typical embryonic stem (ES) cell–like appearance were picked up on approximately days 21 to 28. These cells showed robust stability in phenotype, had high alkaline phosphatase (ALP) activity (Figure 1C), and expressed SSEA-1 at levels comparable with those in ES cells (supplemental Figure 1B). In the absence of leukemia inhibitory factor, they readily formed embryoid bodies (data not shown). By using a single-base polymorphism in *CD45*,[17] we could demonstrate that, of the iPSC clones thus established, 3 were derived from $Ly5.1^+$ cells and 1 from a $Ly5.2^+$ cell (Figure 1D). These results formally demonstrate that direct reprogramming of marrow hematopoietic cells is feasible given that transdifferentiation of HSCs to nonhematopoietic lineage cells is, if it ever occurs, an extremely rare event.[20] We named these iPSCs sHSC-iPS cells (sHSC-iPSCs) specifically when established from BM HSPCs reconstituted from a single HSC.

Each sHSC-iPSC clone was demonstrated to retain proviral sequences of the 4 iPSC factors (supplemental Figure 2A), without detectable transgene expression, probably resulting from gene silencing (supplemental Figure 2B). In contrast, all sHSC-iPSCs were found to express each iPSC factor gene endogenously (supplemental Figure 2B). All sHSC-iPSCs were shown to express the ES cell marker genes *Nanog*, *ERas*, *Rex1*, and *Gdf3* (supplemental Figure 3A). Nanog expression was also confirmed by immunostaining (supplemental Figure 3B). Despite the low expression levels of *Ecat1* and *Zfp296*, another set of ES cell marker genes, these sHSC-iPSCs were shown to

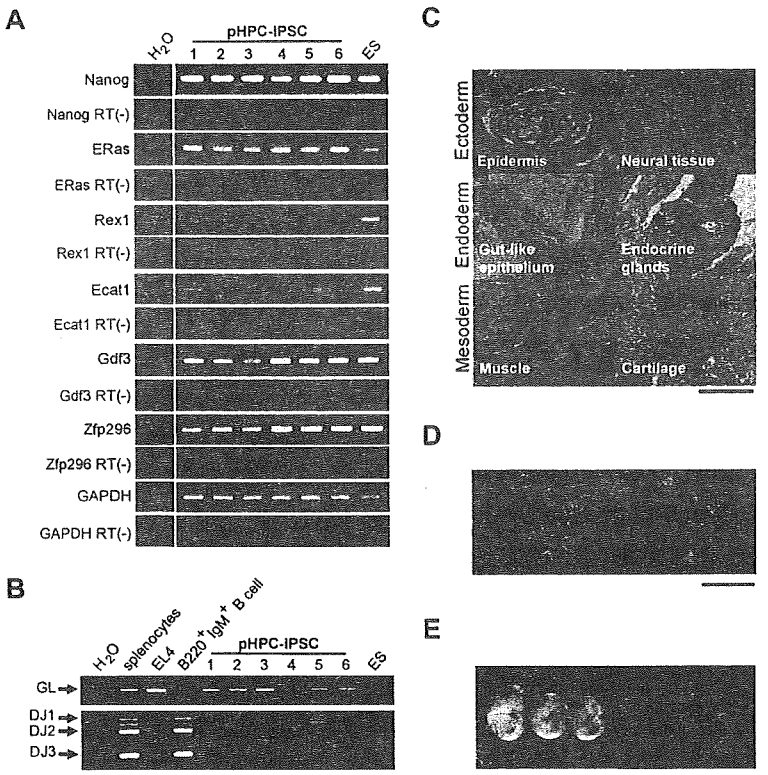

Figure 2. Characterization of primary BM hematopoietic cell–derived iPSCs generated using the 4 iPSC factors. (A) Reverse-transcription PCR analysis showing ES marker gene expression in primary BM HSPC-derived iPSC clones (pHPC-iPSCs). H_2O indicates no-template control; ES, ES cells as a positive control; RT (−), no-reverse-transcriptase control. A vertical line has been inserted to indicate a repositioned gel lane. (B) PCR analysis for Ig gene rearrangement of D-J segments (DJ1-DJ3) in pHPC-iPSC clones. GL indicates amplification of the fragment representing unrearranged, germline configuration of the Ig heavy chain gene; EL4, a T lymphoma cell line as an unrearranged control. (C) Histologic sections of teratomas derived from a pHPC-iPSC clone. (D) Images of pHPC-iPSC colonies derived from an EGFP-transgenic mouse. Bars represent 100 μm (C-D). (E) E10.5 chimeric embryos generated with one representative EGFP+ iPSC clone.

be competent in both teratoma formation (supplemental Figure 4) and contribution to chimeric mice (Figure 1E).

We next sought to confirm the reproducibility of direct reprogramming of primary BM HSPCs. Lin^-Kit^+ BM cells obtained from adult B6 mice were subjected to retrovirus-mediated reprogramming procedures (Figure 1B). From approximately 5×10^5 HSPCs, we consistently obtained approximately 10 to 30 discrete colonies with typical ES cell–like appearances that stained for ALP (data not shown). Interestingly, iPSC clones established from primary BM HSPCs (pHPC-iPSCs) were shown to express ES cell marker genes more robustly than did sHSC-iPSCs (Figures 2A, S3A). Expression levels in endogenous iPSC factor genes were also more intense in pHPC-iPSCs (supplemental Figure 5B) than in sHSC-iPSCs (supplemental Figure 2B). This may support the idea that huge replicative stress imposed on a single HSC by hematopoietic reconstitution might restrict effective reprogramming of target cells, which are thought to be in senescent states. Confirmation of germline configuration in the immunoglobulin gene revealed the non–B-cell origin of pHPC-iPSCs (Figure 2B). pHPC-iPSCs had the potential for multilineage differentiation, as evidenced by the formation of teratomas, which contained various tissues representing all 3 germ layers (Figure 2C). We were also successful in generating pHPC-iPSCs that constitutively expressed green fluorescence protein from enhanced green fluorescent protein (EGFP)–transgenic mice[21] (Figure 2D). These iPSCs showed a high contribution to embryonic development when microinjected into blastocysts (Figure 2E).

Here we report generation of iPSCs from hematopoietic cells with unrearranged immunoreceptor genes by direct viral transfer of iPSC factors. The principle shown here ensures the feasibility of direct reprogramming of human hematopoietic cells, in conjunction with the recent report of iPSC generation from human blood.[8] The defined cellular origin of our iPSCs enables formal comparative studies using iPSC clones from various sources: One intriguing question is whether or not our iPSC clones differ from those generated from other tissues in respect to reprogramming efficiency, genomic stability, ability of tissue differentiation, and susceptibility to tumorigenesis. Another question is what types of cells in murine HSPCs are actually reprogrammed into iPSCs. At present, we have not yet succeeded in iPSC generation from highly purified HSCs. Considering the germline configuration of the immunoglobulin gene in our iPSC clones (Figure 2B) and the fact that the transduced cells rapidly acquired granulocytic/myeloid-lineage marker expression in our culture conditions (data not shown), myeloid progenitors are currently the plausible target cells of iPSC induction in our system. Studies to address all these issues are ongoing.

Acknowledgments

The authors thank S. Yamanaka and K. Takahashi for plasmids, R. C. Mulligan for 293GP and 293GPG cells, and H. Kawamoto and T. Ikawa for help with Ig gene analysis.

This work was supported in part by a grant from the Project for Realization of Regenerative Medicine from the Ministry of Education, Culture, Sports, Science and Technology Japan (H.N.) and by the Global Center of Excellence program from the Ministry of Education, Culture, Sports, Science and Technology Japan.

Authorship

Contribution: M. Okabe generated and characterized iPS cells; M. Otsu generated iPS cells and wrote the manuscript; D.H.A. prepared virus-producing cells; T.K. and Y.W. performed blastocyst injection; Y.M. prepared a single HSC-transplanted chimeric mouse; M. Onodera established transduction procedures